Int. J. Electrochem. Sci., 10 **(2015)** 2239 - 2252

International Journal of
ELECTROCHEMICAL
SCIENCE
www.electrochemsci.org

Microemulsions of Sorbitans and its Derivatives for Iontophoretic Drug Delivery

Vinay K. Singh[1], *Arfat Anis*[2], *S.M. Al-Zahrani*[2] *and Kunal Pal*[1,*]

[1] Department of Biotechnology & Medical Engineering, National Institute of Technology, Rourkela-769008, Odisha, India.
[2] Department of Chemical Engineering, King Saud University, Riyadh-11421, Saudi Arabia.
[*]E-mail: pal.kunal@yahoo.com; kpal.nitrkl@gmail.com

Received: 12 November 2014 / *Accepted:* 25 December 2014 / *Published:* 19 January 2015

This study explains the development and characterization of microemulsions for iontophoretic drug delivery. The microemulsions were developed using a pseudo ternary phase diagram. Biphasic formulations of sesame oil were developed using a mixture of span 80 and tween 80 as surfactant mixture (S_{mix}). The composition of the S_{mix}, sesame oil and water was varied. Microemulsions were formed at a S_{mix} concentration of > 60 %. The formulations were characterized by microscopic studies, FTIR spectroscopy, viscosity, mechanical analysis and impedance analysis. A model drug, metronidazole, was incorporated in the microemulsions to check its drug release behavior. FTIR spectra suggested no interactions amongst the formulation components and the drug. The viscosity and firmness was higher in the microemulsion possessing lower water/surfactant ratio. The microemulsions were electroconductive in nature. The microemulsions showed 42-47 % increase in the amount of metronidazole released under the influence of current as compared to the passive release. The release profile followed zero order release kinetics. The developed microemulsions can be used for iontophoretic drug delivery applications.

Keywords: Microemulsion, sesame oil, impedance spectroscopy, iontophoretic delivery

1. INTRODUCTION

In recent years, iontophoresis has drawn attention of the formulation scientists to deliver the drugs under the influence of low electric current. The synergistic effect is reported when an electric current is applied [1]. The amount of drug released can be enhanced, therefore, iontophoretic delivery may be used in various applications where faster release of drug may add beneficial effects (e.g. dermatological and ocular delivery). The release rate is dependent on various factors which include concentration of drug, raw materials and their respective ratios, amount and duration of applied current

and the surface area of the sample in contact with the electrode. The iontophoretic delivery can be advantageous for the drugs which undergo first pass metabolism [2]. Iontophoresis may be used as targeted delivery system thereby reducing the adverse effects associated with the conventional drug delivery [3]. Gratieri and Kalia (2014) reviewed iontophoresis for targeted delivery of drugs for treating eye and skin diseases [4]. Delgado-Charro (2012) discussed about iontophoresis for delivering the drugs through nail to treat nail diseases such as onychomycosis and psoriasis [5].

Microemulsions are biphasic, homogenous and optically clear formulations. They are inherently thermodynamically stable. The microemulsions can be broadly categorized either as water-in-oil or oil-in-water type based on the solubility of dispersed phase in continuous phase. In general, a hydrophilic surfactant (hydrophilic lipophilic balance i.e. HLB > 10) favors the formation of oil-in-water (O/W) emulsions and a lipophilic surfactant (HLB < 10) favors the formation of water-in-oil (W/O) emulsions [6].

Sorbitans and their derivatives are large group of non-ionic surfactants used exclusively as emulsifying agent in food, pharmaceutical and cosmetics. Span 80 {sorbitan monooleate, [(2R)-2-[(2R,3R,4S)-3,4-dihydroxytetrahydrofuran-2-yl]-2-hydroxy-ethyl] octadec-9-enoate, $C_{24}H_{44}O_6$} and tween 80 {polyoxyethylene (20) sorbitan monooleate, 3,6-anhydro-2,4,5-tris-O-(2-hydroxyethyl)-1-O-{2-[(9E)-octadec-9-enoyloxy]ethyl}hexitol, $C_{185}H_{368}O_{86}$} are used in combination in different ratios to achieve surfactant mixtures with different HLB values for the development of biphasic formulations [7]. Silva *et al.* (2013) reported improved solubility of amphotericin loaded microemulsions using spans and tweens [8]. Mahdi *et al.* (2011) investigated the formation of emulsions and microemulsions using different surfactant combinations of spans and tweens [9]. Sesame oil is obtained from the ripe seed of *Sesamum indicum L.* by cold pressing the sesame seeds. Sesame seeds are reported to contain highest oil (44-58 %) among the other edible oil. It possess anti-inflammatory, anti-tubercular, anti-bacterial and anti-oxidant properties [10].

Metronidazole {2-Methyl-5-nitroimidazole-1-ethanol, $C_6H_9N_3O_3$} is a nitroimidazole antimicrobial used for treating various topical infections [11]. Many scientists reported development of different types of formulations by varying the composition of the oil, emulsifier and water using pseudo-ternary plot [12-14].

In the current study, the phase behaviour of the ternary systems composed of surfactant mixtures (span 80-tween 80 in the ratio of 1:2 w/w), sesame oil and water has been investigated by mapping the pseudo-ternary phase diagram. The composition of the S_{mix} was chosen from the previous studies conducted in-lab [15]. Microemulsions are well explored for their conventional and controlled release application of bioactive agents but are rarely reported for iontophoretic delivery. There is very few reported literature about the use of microemulsions for iontophoretic drug delivery [16]. de Campos Araujo et al. (2010) reported the use iontophoresis for topical delivery of 5-aminolevulinic acid from the microemulsions [17]. Sintov and Brandys-Sitton (2006) reported significant increase in the flux during the short-term iontophoresis application in skin permeation study of lidocaine [18].

The current study details about a simple and the cost-effective method for the development of microemulsions. The microemulsions were characterized by FTIR spectroscopy, mechanical properties and electrical properties. Metronidazole loaded microemulsions were tested as vehicles for iontophoretic drug delivery applications.

2. EXPERIMENTAL

2.1. Materials

Edible grade sesame oil (Tilsona®) was purchased from Recon Oil Industries Ltd., Mumbai, India. Span 80 and tween 80 were supplied by Loba Chemie Pvt. Ltd. and Himedia, Mumbai, India, respectively. Metronidazole was a kind gift from Aarti drugs, Mumbai, India. Millipore water was used throughout the study.

2.2. Methods

2.2.1 Preparation of microemulsions using pseudo-ternary phase diagrams

S_{mix} and sesame oil were weighed accurately in culture vials. They were mixed properly to form a homogenous mixture using an overhead stirrer (500 RPM, 4-5 min). Water phase was added drop-wise to the above mixture with constant stirring for 15 min. A slight foam formation was observed during the preparation which settled down after keeping the formulations undisturbed, overnight. A model antimicrobial drug, metronidazole (1% w/w) was incorporated within the selected microemulsions. The microemulsions were evaluated physically for various organoleptic properties (pH, color, texture and overall appearance). The pH of the microemulsions was measured by dipping the pH measuring probe in the formulations using digital pH meter (EI instruments, Model: 132E, Haryana, India).

2.2.2. Microscopic studies

The type of the microemulsion (oil-in-water or water-in-oil) formed and their internal structures were analyzed by fluorescence microscope (Optika, XDS-3FL, Italy). 0.1% fluoral yellow was dissolved in sesame oil for preparing the samples for fluorescence microscopy [19].

2.2.3. Mechanical properties

The viscosity of the microemulsions was measured as a function of shear rate (25 to 100 s^{-1} and 100 to 25 s^{-1}) at room-temperature using a cone-and-plate viscometer (Bohlin visco 88, Malvern, UK) [20].

The mechanical properties of the microemulsions were further evaluated using static mechanical tester (Stable Microsystems, TA-HDplus, U.K.) [21]. The study using static mechanical tester was performed according to the protocol shown in Table 1.

Table 1. Test parameters for macro-scale deformation studies

Type of study	Type of fixture	Testing conditions			Mode of study
		Pre test speed (mm/sec)	Test speed (mm/sec)	Post test speed (mm/sec)	
Stress relaxation	HDP/SR spreadability rig with 45° conical perspex probe	1.0	0.5	10.0	Auto force (5g; 5 mm)
Spreadability	HDP/SR spreadability rig with 45° conical perspex probe	2.0	2.0	2.0	Button mode Distance (23 mm)
Backward extrusion*	A/BE back extrusion rig	1	1	1	Button mode Distance (20 mm)

*The test was performed using a flat probe (perpex made) of 40 mm diameter in a 50 ml beaker (inner diameter: 42 mm), filled ~75% of its volume.

The relative viscosity of the microemulsions was calculated using backward extrusion study conducted at 37 °C. Water was taken as reference. The apparent dynamic viscosity of water was taken as 0.693 mPa.s at 37 °C. The relative viscosity of the microemulsions was calculated using the following equation [14].

$$\eta_{Sample} = \eta_{Water} \frac{(df/dx)_{Sample}}{(df/dx)_{Water}} \quad (1)$$

where, η is the viscosity, df/dx is the slope of the force *vs.* distance curve of backward extrusion profile when the probe is pulled back.

2.2.4. Electrical properties

The electrical properties of the microemulsions were measured using an impedance analyzer (Phase sensitive multimeter, PSM1735, Numetriq, Japan). A set of copper electrodes was used to record the impedance parameters such as impedance, phase angle, capacitance and loss tangent as a function of frequency (0.1Hz–1MHz) at room temperature [1-3].

2.2.5. Iontophoretic drug delivery

Metronidazole (model drug) loaded microemulsions were investigated for the possible application of the microemulsions in iontophoretic drug delivery. An in-house developed iontophoretic drug delivery setup was used for the study. The release study was performed in both active (electrically mediated) and passive form (non-electrically mediated). The effect of electric current on the release profile was analyzed by comparing the amount of drug released during active and passive release study. The study was performed according to the protocol described elsewhere [1]. In short, accurately

weighed (2 g) drug containing microemulsions were taken in the donor compartment where as the receptor compartment contained approximately 25 ml of the dissolution media (distilled water, 37 ^{o}C, 100 rpm). The donor and the receptor compartments were connected using stainless steel electrodes (diameter 1.4 cm). An a.c. current (32.13 μA, I_{rms}) supplying a current density of 20.88 μA/cm^2 was used during the study. A standard signal generator was used to generate a sinusoidal voltage of 0.707 V (V_{rms}) using a constant current source. The release of metronidazole from the microemulsions was checked for 2 h by analyzing the releasates collected on regular time intervals (0.25, 0.5, 0.75, 1, 1.5 and 2h). 3 ml of the releasate was pipette out and subsequently replaced with fresh dissolution media to maintain the overall dissolution media to 25 ml. The releasates were analyzed spectroscopically (UV 3200 double beam, Labindia) at 321 nm and the cumulative percent drug release was calculated [22-23].

3. RESULTS AND DISCUSSIONS

3.1. Preparation of formulations

The pseudo-ternary phase diagram showed formation of microemulsions in the area where the S_{mix} proportions was very high and the sesame oil proportions was very low (Figure 1). The microemulsions were yellowish in color due to the presence of higher proportion of S_{mix}. Though they possessed very low water/surfactant ratio, the presence of higher proportions of S_{mix} indicated that the formulations might be thermodynamically very stable. This is due to the fact that at this high concentration of S_{mix}, the interfacial tension is reduced to a great extent which prevents the coalescence of the dispersed phase [24]. The formation of microemulsions using different non-ionic S_{mix}, edible oil system and water has been reported elsewhere [25-26]. Two formulations were selected randomly from the area where microemulsion formation took place and were characterized thoroughly (Table 2).

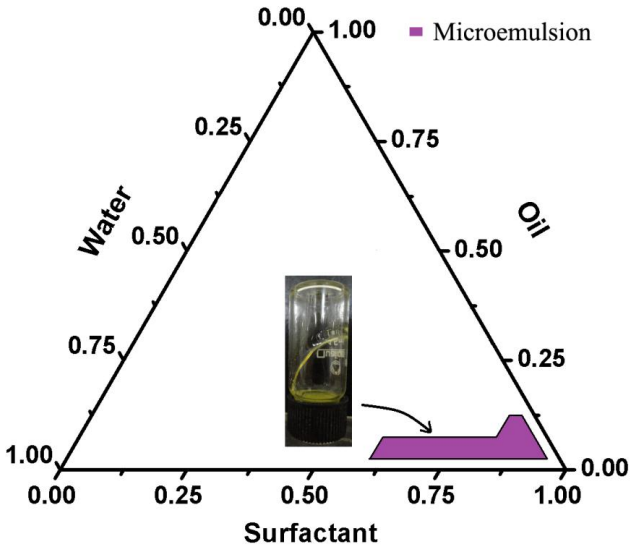

Figure 1. Pseudo-ternary phase diagram depicting area of microemulsion formation.

Table 2. Composition of the microemulsions

Formulations	Surfactant mixture (% w/w)	Sesame oil (% w/w)	Water (% w/w)	Metronidazole (% w/w)	Water/Surfactant ratio
ME1	87.5	2.5	10	-	0.114
ME1M	87.5	2.5	9	1	-
ME2	80	10	10	-	0.125
ME2M	80	10	9	1	-

3.2. Microscopic studies

The internal structure and the exact arrangement of the phases (oil and water) were studied by the fluorescent microscopy. Microemulsions showed presence of densely packed droplets dispersed throughout the continuous phase. Also, they showed the presence of randomly arranged fibrous structures, suggesting their bicontinuous nature (Figure 2).

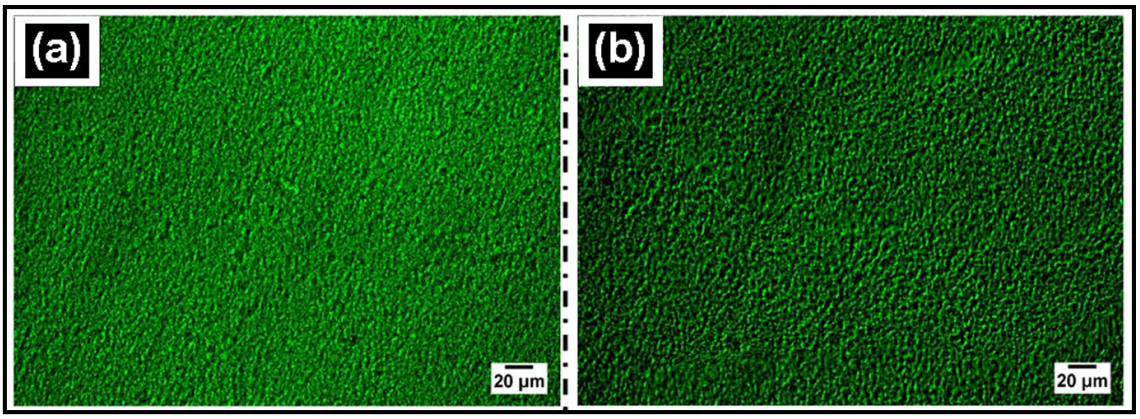

Figure 2. Fluorescent microscopy of the microemulsions (a) ME1, and (b) ME2.

3.3. FTIR spectroscopy

The absorption peaks obtained in FTIR spectrum of the microemulsions were in exact match with the FTIR spectra of the raw materials provided in the literature [27-28]. All the characteristic peaks of the raw materials were conserved in the blank as well as the drug loaded microemulsions (Figure 3). This suggested that no significant structural changes occurred in the formulation components at the molecular level. Few peaks were slightly shifted and may be due to the changes in the immediate environment of the functional groups when the microemulsions were prepared.

All the formulations showed a broad peak in the range of 3350-3450 cm^{-1} which is associated with the formation of intermolecular hydrogen bonding amongst the formulation components [29]. The major absorption peak at ~2920 cm^{-1} was due to the asymmetric stretching vibration of C-H bond (CH_2) of alkane moiety [30]. Absorption peaks at ~1740 cm^{-1} and at ~ 1090 cm^{-1} indicated the

presence of stretching vibration due to the ester group of triglycerides present in sesame oil [31]. The less intense absorption peaks observed at 1460 cm^{-1} and 1373 cm^{-1} were due to CH_2 and CH_3 scissoring vibrations, respectively [32]. Metronidazole loaded formulations did not show any extra peak which may be associated to very small quantity of metronidazole present in the formulations.

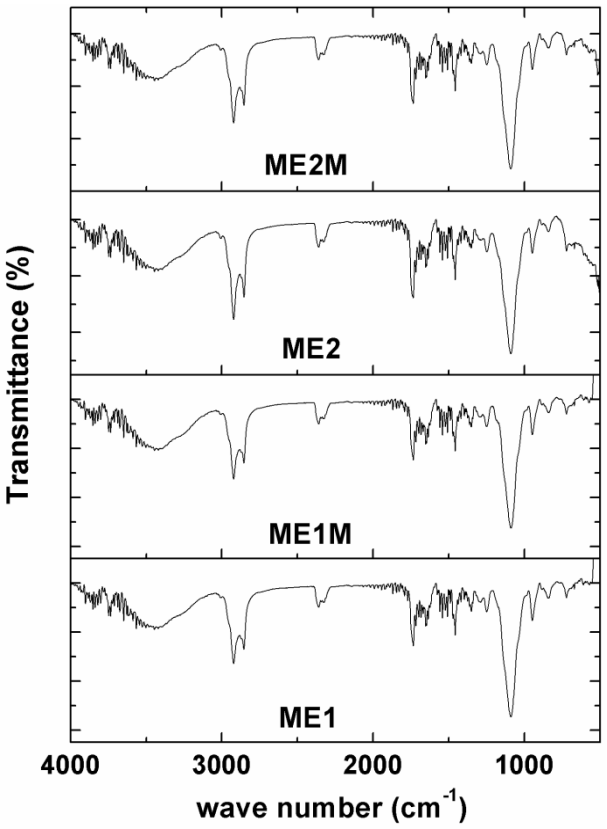

Figure 3. FTIR spectra of microemulsions.

3.4. Mechanical properties

The viscosity analysis showed a decrease in the viscosity with the increase in shear rate. This indicated non-Newtonian shear-thinning behavior of the microemulsions (Figure 4a). ME1 possessed higher apparent viscosity compared to ME2 which may be associated to its higher water/surfactant ratio.

The backward extrusion profile suggested Newtonian flow behavior of the MEs (Figure 4b). This is in contrary to the results obtained from the viscosity studies. This observation may be explained by the fact that the viscosity study provides mechanical information on a small scale deformation basis and may help divulging information on the particle-particle interactions. Viscosity analysis is more sensitive than the large scale deformation test (using a static mechanical tester). Due to this reason, the relative viscosity determined using mechanical tester was not able to determine the particle-particle interactions and indicated Newtonian flow behavior.

The viscoelastic property of the microemulsions was studied by analyzing their stress relaxation profiles (Figure 4c-d). During the study, the probe was allowed to move a distance of 5 mm after detecting a 5.0 g of force. The force value increased with the movement of probe. The highest force value is named as F_0. The probe was kept at the same distance for 60 sec. The force value decreased and reached to a plateau named as residual force, F_r [33]. Percent stress relaxation of the formulations was calculated using the formula given below [34].

$$\%\ relaxation = \left(\frac{F_0 - F_r}{F_0} \right) \times 100 \quad (2)$$

The % stress relaxation of the ME1 and ME2 was ~41 and ~46 %, respectively suggesting viscoelastic nature of the microemulsions (Figure 4c-d, Table 3) [35]. Viscoelastic properties of the microemulsions was further confirmed by normalizing the force-time data using modified Peleg's equation [36].

$$\frac{\left(F_0 - F(t)\right)t}{F_0} = k_1 + k_2 t \quad (3)$$

where; k_1 and k_2 indicate the initial rate and the extent of the relaxation, respectively.

The area under the curve (S^*) of the normalized force-time graph gives information about the viscoelastic property of the formulations. The S^* value for the microemulsions was ~ 0.37 which also suggested that the developed microemulsions were viscoelastic in nature (Table 3).

Table 3. Mechanical properties of the formulations

Samples	**Stress relaxation studies**						**Spreadability studies**	**Relative viscosity (mPa.s)**
	Un-normalized curve			Normalized curve			Firmness (g)	
	F_0 (g)	F_r (g)	% relaxation	k_1	k_2	S^* (g.sec)		
ME1	7.62 ± 0.18	4.1 ± 0.14	46.29 ± 1.27	0.0257	0.038	0.37614	34.96 ± 1.53	0.62 ± 0.02
ME2	7.61 ± 0.21	4.48 ± 0.11	41.19 ± 1.52	0.0247	0.039	0.37611	29.39 ± 1.27	0.59 ± 0.03

The non-linear viscoelastic behavior of microemulsions was further analyzed by fitting the stress relaxation data using Wiechert mathematical model. Wiechert model describes viscoelastic behavior of the material using a combination of spring and dashpot elements [37]. The addition of the three spring-dashpot elements satisfactorily explained the viscoelastic behavior of the microemulsions (insert, Figure 4e) [38]. Mathematically, Wiechert model is defined using equation 4 [38].

$$P_{(t)} = P_0 + P_1 e^{-t/\tau_1} + P_2 e^{-t/\tau_2} + P_3 e^{-t/\tau_3} \quad (4)$$

where, P(t) is the magnitude of the decaying stress at time t; P_0 is the magnitude of the residual stress; P_1, P_2 and P_3 are the relaxation modulus of the spring; τ_1, τ_2 and τ_3 are the relaxation time of the dashpot during the stress relaxation test.

Table 4. Stress relaxation model fitting using Wiechert model

Formulations	Stress relaxation model	R^2 (%)
ME1	$P_{(t)} = 5.10 + 0.95.e^{-t/0.034} + 0.94.e^{-t/0.034} + 1.58.e^{-t/0.034}$	0.931
ME2	$P_{(t)} = 5.21 + 0.99.e^{-t/0.007} + 0.87.e^{-t/0.007} + 0.66.e^{-t/0.007}$	0.930

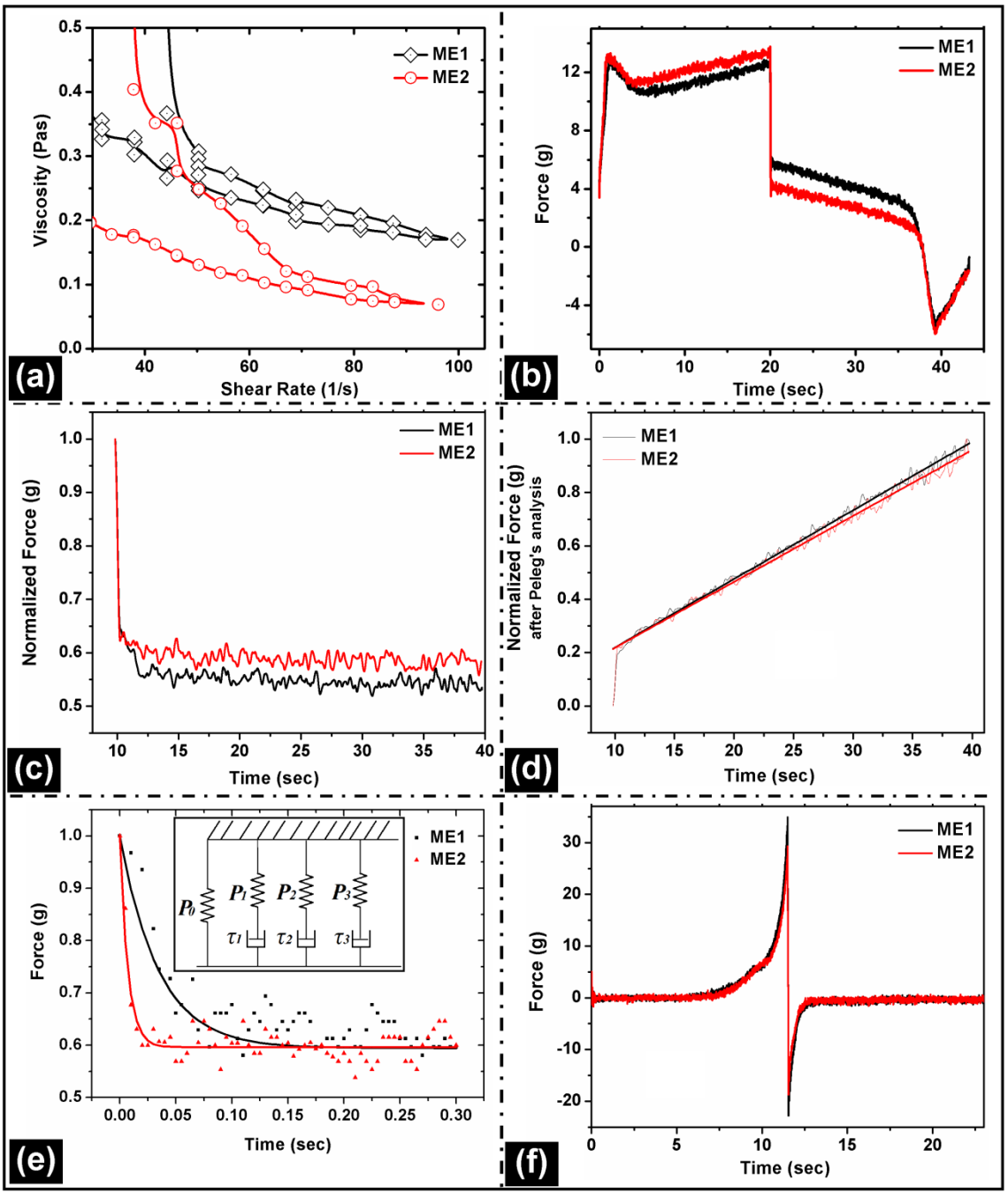

Figure 4. Mechanical properties of the microemulsions (a) viscosity studies, (b) backward extrusion studies; stress relaxation studies (c) normalized force-time curve, (d) normalized force-time curve after Peleg's analysis; (e) Wiechert model fitting (schematic representation of the model as insert) and (f) spreadabilty studies.

The fitting of the relaxation modulus curve of the Wiechert model and the experimental data obtained from the stress relaxation test has been shown in Figure 4e. The fitting was done using least-square difference regression method in Microsoft Excel 2007. Solver add-in was used to determine the best-fit. The correlation coefficient between the experimental and the mathematical model was found to be ~0.93 in both the cases (Table 4). Also, it was clear from the model fitting that ME1 and ME2 showed almost similar P_0, P_1, and P_2 values but P_3 value and relaxation modulus values (τ_1, τ_2 and τ_3) showed significant difference. It was higher in ME1 compared to ME2 which suggested its firmer nature.

The firmness of the microemulsions was determined by the spreadability profile. The firmness of a formulation is inversely related to the spreadabilty. This is indicated by the peak positive force of the force-time plot of the spreadability profile [39]. ME1 showed higher firmness compared to ME2 (Figure 4f, Table 3). The result was in relation to the viscosity profiles obtained from the cone-and-plate viscometer.

3.5. Electrical properties

The electrical behavior of the microemulsions was studied to explore their conductivity profiles. Nyquist plot (-Z'' vs. Z') showed two well-defined regions. A semicircle was obtained at higher frequencies which is associated with the bulk effect of the electrolytes. At lower frequencies, the formulations showed the presence of a non-vertical spike due to the roughness at the electrode-electrolyte interface (Figure 5a) [40-41]. An electrical equivalent circuit was proposed to model the Nyquist plot. The bulk resistance (R_b) of the formulations was obtained by fitting the data using EIS Spectrum Analyser [41]. Both microemulsions showed almost similar R_b values. ME1 showed a slightly higher R_b values compared to ME2. The result was in relation to the mechanical properties of the formulations. A CPE element was added in the equivalent circuit to overcome the inhomogeneity of the system (Insert, Figure 5a) [42]. Here, two constant phase elements were added in the equivalent circuit (CPE1 and CPE2). The CPE is placed parallel to a resistor when a depressed semicircle is obtained in Nyquist plot. The high frequency semicircle is represented by the parallel combination of bulk resistance and CPE2 and the non-vertical spike is represented by CPE1. The fitting of the Nyquist plot indicated a good fit.

The a.c. conductivity ($б_{ac}$) of the microemulsions was determined at varied frequencies (Figure 5b). It was inversely related to the R_b values i.e. ME2 showed higher a.c. conductivity compared to ME1. Two regions were observed. The frequency dependent dispersion region was associated to the space charge polarization at the sample-electrode interface. The frequency independent plateau region may be assigned to the bulk conductivity of the formulations [43-44]. This plateau gives information about the d.c. conductivity of the formulations.

The d.c. conductivity of the microemulsions was calculated using the following formula (Table 5):

$$\sigma_0 = (1/R_b) * (l/A) \quad (5)$$

where, l is the thickness and A is the area of the sample. The results were in the same order to the results obtained from a.c. conductivity.

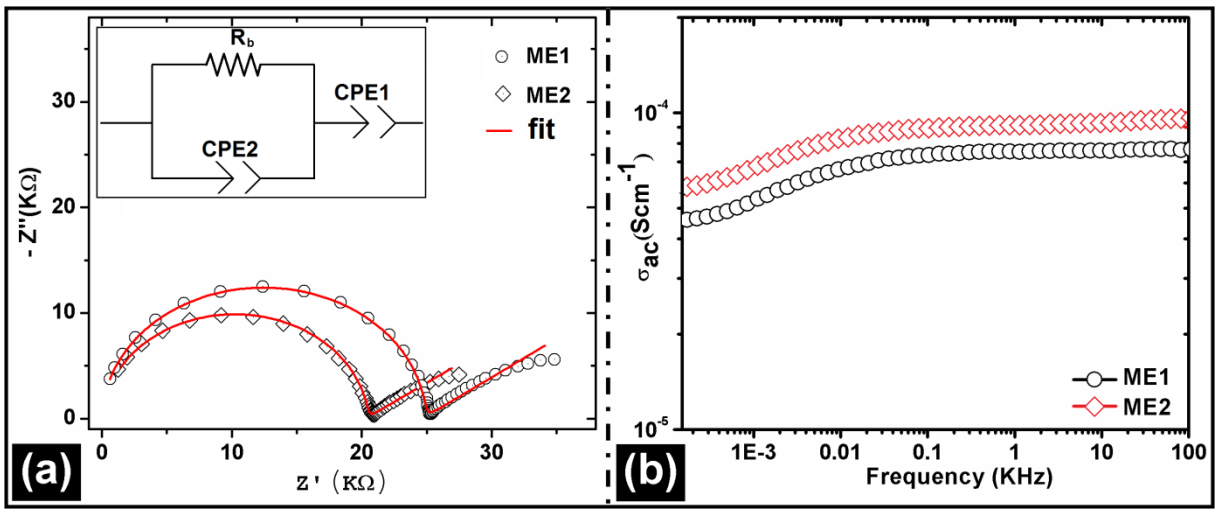

Figure 5. Electrical properties of the microemulsions (a) Nyquist plot (equivalent circuit diagram shown as insert), and (b) a.c. conductivity.

Table 5. Electrical properties of the microemulsions

Formulations	R_b (Ω) (10^4)	$б_{dc}$ (Scm^{-1}) (10^{-5})
ME1	2.47	6.83
ME2	2.03	8.65

3.6. Iontophoretic drug delivery

The electro-conductive nature of the microemulsions indicated that the developed microemulsions can be used in iontophoretic drug delivery. Iontophoresis is based on the release of the drug by applying an electric field on the charged drug molecule [3]. Both ME1M and ME2M showed ~89.5 and ~92 % of the drug released, respectively in 2 h under active condition. The release of drug was quite low under passive condition (~60 and 61 % from ME1M and ME2M, respectively in 2h) compared to the active condition. Though, the difference in the drug release was not significant, ME2M showed higher release of metronidazole compared to ME1M in both active and passive conditions (Figure 6a). Being slightly hydrophilic in nature, the amount of metronidazole released was higher in ME2M. The higher release in ME2M is associated to its higher water/surfactant ratio compared to ME1M. The release rate was higher in active condition compared to the passive condition due to the presence of electrical field. The application of externally applied electrical field resulted in significant increase in drug release percent. The percent increase in the amount of metronidazole released from ME1M and ME2M over a period of 2 h was ~47 and ~42 %, respectively (Figure 6b).

The results were very promising and widen the applicability of the developed microemulsions as carriers for iontophoretic drug delivery.

Different release kinetics models were fitted to the 60 % of the released data. The release of metronidazole showed fitted best to zero-order kinetics. This indicated diffusion mediated concentration independent release of the drug from the microemulsions (Figure 6c).

The diffusion coefficient (n) value of the drug release was calculated by fitting the release data with Korsmeyer-Peppas model (Figure 6d, Table 6). The n-value of ME1M and ME2M was 0.79 and 0.83, respectively. This suggested non-Fickian diffusion of metronidazole [45].

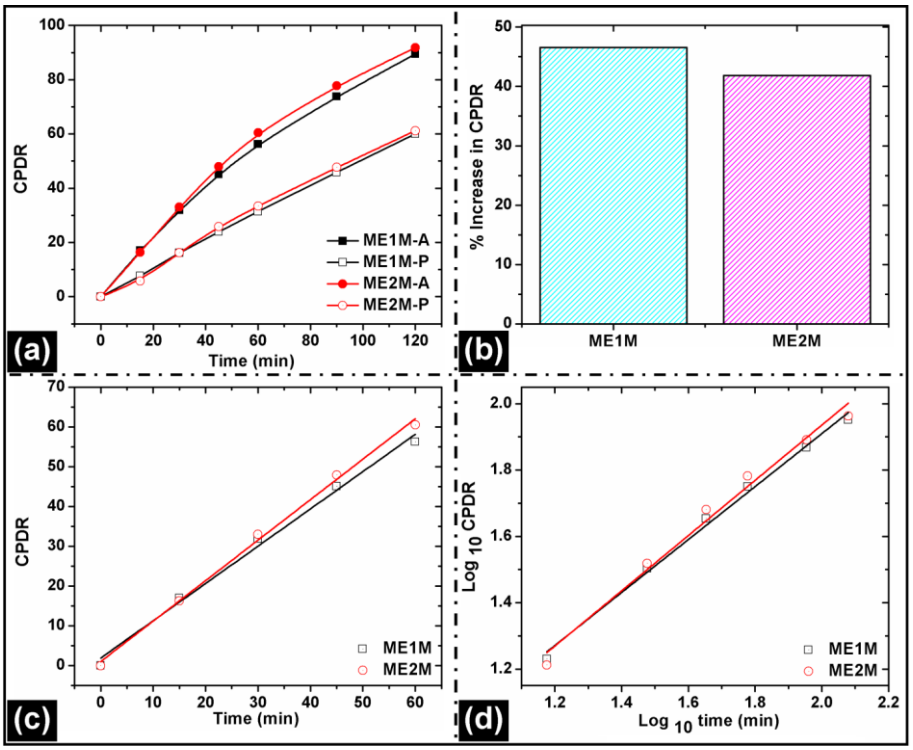

Figure 6. Iontophoretic drug delivery studies (a) cumulative percent drug release under active (A) and passive (P) conditions, (b) increase in amount of drug release under influence of current, (c) zero order release kinetics, and (d) KP model fitting.

Table 6. Iontophoretic drug delivery studies of the developed microemulsions

Formulations	ME1M	ME2M
CPDR		
Active	89.46 ± 3.25	91.78 ± 3.12
Passive	60.02 ± 2.89	61.18 ± 1.28
Zero order		
Adj.R-Square	0.991	0.996
KP Model		
Adj. R-Square	0.993	0.982
n-value	0.79	0.83

4. CONCLUSION

This study explained the development of microemulsions across length scale by varying the composition of S_{mix}, sesame oil and water. Microemulsions were formed at very high concentration of S_{mix} (> 60%). The microemulsions were bicontinuous in nature. FTIR spectra indicated formation of intermolecular hydrogen bonding. Stress relaxation study suggested viscoelastic nature of the microemulsions. The microemulsions possessing higher water/surfactant ratio showed lower viscosity, firmness and conductivity. Metronidazole loaded microemulsions showed 42-47 % increase in the amount of drug released under the influence of current. The release profile followed zero order release kinetics. In gist, the microemulsions can be used as vehicles for iontophoretic delivery of bioactive agents.

ACKNOWLEDGEMENT
The authors acknowledge the support provided by National Institute of Technology, Rourkela for the completion of this study. The authors would like to extend their sincere appreciation to the Deanship of Scientific Research at King Saud University for its funding of this research through the Research Group Project No. RGP-095.

References

1. V. K. Singh, A. Anis, S. Al-Zahrani, D. K. Pradhan, and K. Pal, *Int J Electrochem Sci*, 9 (2014) 5640.
2. D.-H. Oh, K.-H. Chun, S.-O. Jeon, J.-W. Kang, and S. Lee, *Eur J Pharm Biopharm*, 79 (2011) 357.
3. V. K. Singh, A. Anis, S. Al-Zahrani, D. K. Pradhan, and K. Pal, *Int J Electrochem Sci*, 9 (2014) 5049.
4. T. Gratieri, and Y. N. Kalia (2014) Topical Iontophoresis for Targeted Local Drug Delivery to the Eye and Skin. Focal Controlled Drug Delivery: Springer. pp. 263.
5. M. B. Delgado-Charro, *Expert Opin Drug Deliv*, 9 (2012) 91.
6. W. Li, Y. Yu, M. Lamson, M. S. Silverstein, R. D. Tilton, and K. Matyjaszewski, *Macromolecules*, 45 (2012) 9419.
7. J. Jiao, and D. J. Burgess, *AAPS PharmSciTech*, 5 (2003) 62.
8. A. E. Silva, G. Barratt, M. Chéron, and E. Egito, *Int. J. Pharm*, 454 (2013) 641.
9. E. S. Mahdi, M. H. Sakeena, M. F. Abdulkarim, G. Z. Abdullah, M. A. Sattar, and A. M. Noor, *Drug Des Devel Ther*, 5 (2011) 311.
10. W. Wei, X. Qi, L. Wang, Y. Zhang, W. Hua, D. Li, H. Lv, and X. Zhang, *BMC genomics*, 12 (2011) 451.
11. S. Löfmark, C. Edlund, and C. E. Nord, *Clin. Infect. Dis.*, 50 (2010) S16.
12. G. Espinosa, and M. Scanlon, *Food Res Int*, 53 (2013) 49.
13. Z. Wang, and R. Pal, *J Surfactants Deterg*, 17 (2014) 49.
14. S. Pradhan, S. S. Sagiri, V. K. Singh, K. Pal, S. S. Ray, and D. K. Pradhan, *J Appl Polym Sci*, 131 (2014)
15. S. S. Sagiri, B. Behera, T. Sudheep, and K. Pal, *Des Monomers Polym*, 15 (2012) 253.
16. G. Russell-Jones, and R. Himes, *Expert Opin Drug Deliv*, 8 (2011) 537.
17. L. M. P. de Campos Araújo, J. A. Thomazine, and R. F. V. Lopez, *Eur J Pharm Biopharm*, 75 (2010) 48.

18. A. C. Sintov, and R. Brandys-Sitton, *Int. J. Pharm.*, 316 (2006) 58.
19. V. K. Singh, A. Anis, I. Banerjee, K. Pramanik, M. K. Bhattacharya, and K. Pal, *Mat Sci Eng* C, 44 (2014) 151.
20. V. K. Singh, K. Pramanik, S. S. Ray, and K. Pal, *AAPS PharmSciTech*, just accepted (2014).
21. V. K. Singh, I. Banerjee, T. Agarwal, K. Pramanik, M. K. Bhattacharya, and K. Pal, *Colloids Surf B Biointerfaces*, just accepted (2014).
22. V. Vamathevan, R. Amal, D. Beydoun, G. Low, and S. McEvoy, *J Photoch Photobio* C, 148 (2002) 233.
23. K. Pal, A. Banthia, and D. Majumdar, *AAPS PharmSciTech*, 8 (2007) E142.
24. S. S. Sagiri, B. Behera, K. Pal, and P. Basak, *J Appl Polym Sci*, 128 (2013) 3831.
25. H. E. Mize, A. J. Lucio, C. J. Fhaner, F. S. Pratama, L. A. Robbins, and D. S. Karpovich, *J Agric Food Chem*, 61 (2013) 1319.
26. J. Rao, and D. J. McClements, *Food Hydrocolloids*, 25 (2011) 1413.
27. S. F. Sim, and W. Ting, *Talanta*, 88 (2012) 537.
28. X. Shan, L. Chen, Y. Yuan, C. Liu, X. Zhang, Y. Sheng, and F. Xu, *J Mater Sci-Mater* M, 21 (2010) 241.
29. J. Israelachvili, *Colloid Surface* A, 91 (1994) 1.
30. S. Ifuku, Y. Tsujii, H. Kamitakahara, T. Takano, and F. Nakatsubo, *J Polym Sci A Polym Chem*, 43 (2005) 5023.
31. M. Pérez-Mateos, P. Montero, and M. C. Gómez-Guillén, *Food Hydrocolloids*, 23 (2009) 53.
32. D. Atek, and N. Belhaneche-Bensemra, *Eur Polym J*, 41 (2005) 707.
33. H. Drissi-Alami, M. Aroztegui, G. Lemagnen, D. Larrouture, and L. Casahoursat, *J Pharm Belg*, 48 (1993) 43.
34. F. Ebba, P. Piccerelle, P. Prinderre, D. Opota, and J. Joachim, *Eur J Pharm Biopharm*, 52 (2001) 211.
35. G. Bellido, and D. Hatcher, *J. Food Eng*, 92 (2009) 29.
36. M. Peleg, *J Food Sci*, 44 (1979) 277.
37. Gorji Chakespari, A. Rajabipour, and H. Mobli, *Adv J Food Sci Tech*, 2 (2010) 200.
38. Machiraju, A. V. Phan, A. W. Pearsall, and S. Madanagopal, *Comput Meth Prog Bio*, 83 (2006) 29.
39. M. Xu, D. Ivey, Z. Xie, W. Qu, and E. Dy, *Electrochim Acta*, 97 (2013) 289.
40. A. S. Hamdy, E. El-Shenawy, and T. El-Bitar, *Int J Electrochem Sci*, 1 (2006) 171.
41. D. K. Pradhan, R. Choudhary, B. Samantaray, A. K. Thakur, and R. Katiyar, *Ionics*, 15 (2009) 345.
42. V. Baglio, M. Girolamo, V. Antonucci, and A. Aricò, *Int J Electrochem Sci*, 6 (2011) 3375.
43. D. K. Pradhan, R. Choudhary, and B. Samantaray, *Express Polym Lett*, 2 (2008) 630.
44. D. K. Pradhan, B. Samantaray, R. Choudhary, and A. K. Thakur, *J Mater Sci-Mater* El, 17 (2006) 157.
45. S. Dash, P. N. Murthy, L. Nath, and P. Chowdhury, *Acta Pol Pharm*, 67 (2010) 217.